Discrete breathers in anisotropic ferromagnetic spin chains



2001 J. Phys. A: Math. Gen. 34 10839

(http://iopscience.iop.org/0305-4470/34/49/307)

INSTITUTE OF PHYSICS PUBLISHING JOURNAL OF PHYSICS A: MATHEMATICAL AND GENERAL

J. Phys. A: Math. Gen. **34** (2001) 10839–10858 PII: S0305-4470(01)23790-1

# Discrete breathers in anisotropic ferromagnetic spin chains

**J M Speight**[1] **and P M Sutcliffe**[2]

[1] Department of Pure Mathematics, University of Leeds, Leeds LS2 9JT, UK
[2] Institute of Mathematics, University of Kent at Canterbury, Canterbury CT2 7NF, UK

E-mail: J.M.Speight@leeds.ac.uk and P.M.Sutcliffe@ukc.ac.uk

Received 9 April 2001, in final form 3 October 2001
Published 30 November 2001
Online at stacks.iop.org/JPhysA/34/10839

**Abstract**

We prove the existence of discrete breathers (time-periodic, spatially localized solutions) in weakly coupled ferromagnetic spin chains with easy-axis anisotropy. Using numerical methods we then investigate the continuation of discrete breather solutions as the intersite coupling is increased. We find a band of frequencies for which the one-site breather continues all the way to the soliton solution in the continuum. There is a second band, which abuts the first, in which the one-site breather does not continue to the soliton solution, but a certain multi-site breather does. This banded structure continues, so that in each band there is a particular multi-site breather which continues to the soliton solution. A detailed analysis is presented, including an exposition of how the bifurcation pattern changes as a band is crossed. The linear stability of breathers is analysed. It is proved that one-site breathers are stable at small coupling, provided a non-resonance condition holds, and an extensive numerical stability analysis of one-site and multisite breathers is performed. The results show alternating bands of stability and instability as the coupling increases.

PACS numbers: 05.45.Xt, 05.50.+q, 05.45.YV, 63.20.Pw, 75.10.-b

## 1. Introduction

Discrete breathers are time periodic, spatially localized solutions in networks of coupled oscillators (including rotors and spins). They arise in a variety of very general systems [13, 16] due to the interplay between nonlinear and discrete effects, and therefore there is an enormous potential for their application in many areas of physics, particularly condensed matter and biophysics, where physical systems are often inherently discrete. Generally one finds that as the system is moved closer to its continuum limit, by increasing a coupling constant in the theory, there comes a point at which a discrete breather solution no longer exists. This is to be expected since an increase in the coupling constant results in an expansion of the phonon

  

frequency band and eventually this band captures a harmonic of the breather frequency. In fact, it is often the case that the discrete breather cannot be continued even up to the point at which the above resonance argument applies, and this is not well understood.

In this paper we study the classical equations of motion for a ferromagnetic spin chain with an easy-axis anisotropy. Some numerical studies of discrete breathers (which are known as intrinsic localized modes in the condensed matter physics literature) have been performed in the cases of easy-plane ferromagnets [17] and easy-axis antiferromagnets [12]. However, both the perspective and the results of the current investigation are quite different. We prove the existence of discrete breathers in the weakly coupled case by starting from the anti-continuum limit (zero coupling constant) and applying an implicit function theorem argument to the trivial one-site breather. We then apply numerical methods to investigate the continuation of this solution as the coupling constant is increased, with the novel result that it continues for all values of the coupling. This is explained by an examination of the spin waves. Depending upon the breather frequency, the continuation results in either the soliton solution of the continuum model or a trivial static solution in which all spins are either aligned or anti-aligned with the vacuum. Similar results are found to apply to multi-site breathers, which fit into an intricate pattern, and lead us to conjecture that the continuum soliton solution (of any allowed frequency) can always be obtained from the continuation of a particular form of multi-site breather. Evidence in support of this conjecture is presented. The numerical results are in some ways reminiscent of those found [5, 10] for the discrete nonlinear Schrödinger (DNLS) system, but have not previously been seen in spin chains.

We then go on to perform a linear stability analysis of the breathers within the Krein theory framework pioneered by Aubry [1]. We prove that nonresonant continued one-site breathers must be stable for sufficiently weak coupling, and numerically investigate the stability of both one-site and multisite breathers. The results suggest that those families which tend to the continuum soliton experience regular repeating bands of instability of diminishing strength as the coupling increases.

During the refereeing process for this paper, a very interesting paper by Flach *et al* [9] on breathers in very similar systems appeared. The differences between their results and ours are, briefly, as follows. They consider both easy-axis and easy-plane anisotropy, but in the case where the exchange interaction is anisotropic also (our exchange interaction maintains isotropy). Breather existence is proved by continuing from a limit in which two of the exchange integrals vanish, but the third remains nonzero. Since the continuation is for small values of the continuation parameters (the two small exchange integrals) their existence result applies to strongly anisotropic exchange interaction, as opposed to ours, which applies to isotropic exchange. More importantly, in this paper we exploit the isotropic exchange to reduce the breather equations to a purely algebraic system, which greatly simplifies the analysis in comparison with theirs. Consequently our existence result requires none of the nonresonance hypotheses of Flach *et al* 's. Also we are able to build spatial localization of breathers directly into our analysis, whereas Flach *et al* do not consider this issue at all (although standard results of MacKay on exponential breather localization should apply to their system just as they do to ours—see section 3). Similarly, we exploit the exchange isotropy to simplify the linear stability analysis, again reducing it to a purely algebraic problem, a reduction not possible for the systems analysed in [9]. We are able, therefore, to perform a very detailed numerical existence and stability analysis at minimal computational cost. To summarize, Flach *et al* prove a result of rather more general applicability and physical relevance than ours, though their context does not, strictly speaking, include ours. We consider a somewhat more idealized system, but obtain correspondingly stronger results.

## 2. Anisotropic ferromagnetic spin chains

The classical formulation of a spin chain involves a three-component unit vector $\boldsymbol{n}_i$, giving the spin at each lattice site $i \in \mathbb{Z}$. The type of spin chain is defined by its Hamiltonian, which we take to be

$$H = \sum_i \left\{ \alpha(1 - \boldsymbol{n}_i \cdot \boldsymbol{n}_{i+1}) + \frac{A}{2}[1 - (\boldsymbol{n}_i \cdot \boldsymbol{e}_3)^2] \right\}. \tag{2.1}$$

Here $\alpha \geqslant 0$ is the coupling constant (exchange integral), which is positive in the case of a ferromagnet, and $A > 0$ is the anisotropy constant, which is also positive since we wish to consider an easy-axis anisotropy, with $\boldsymbol{e}_3 = (0, 0, 1)$ being the easy axis. In this case the minimum of the Hamiltonian is zero, obtained by the vacuum configuration $\boldsymbol{n}_i = \pm\boldsymbol{e}_3$. In the following we shall choose $+\boldsymbol{e}_3$ to be the vacuum configuration and refer to spins which take the values $+\boldsymbol{e}_3$ and $-\boldsymbol{e}_3$ as being spin up and down respectively. Furthermore, by applying a scaling symmetry we can, without loss of generality, set $A = 1$.

The equation of motion is obtained from the Hamiltonian as

$$\dot{\boldsymbol{n}}_i = -\boldsymbol{n}_i \times \frac{\partial H}{\partial \boldsymbol{n}_i} \tag{2.2}$$

where a dot denotes differentiation with respect to time. Using (2.1) we obtain

$$\dot{\boldsymbol{n}}_i = \alpha \boldsymbol{n}_i \times (\boldsymbol{n}_{i+1} + \boldsymbol{n}_{i-1}) + (\boldsymbol{n}_i \cdot \boldsymbol{e}_3)(\boldsymbol{n}_i \times \boldsymbol{e}_3). \tag{2.3}$$

Discrete breather solutions have the form

$$\boldsymbol{n}_i(t) = (\sin\theta_i \cos\omega t, -\sin\theta_i \sin\omega t, \cos\theta_i) \tag{2.4}$$

where $\omega$ is the frequency. Substituting this ansatz into the equation of motion (2.3) yields the following nonlinear second-order difference equation for the angles $\theta_i$:

$$\alpha\{\cos\theta_i(\sin\theta_{i+1} + \sin\theta_{i-1}) - \sin\theta_i(\cos\theta_{i+1} + \cos\theta_{i-1})\} = \sin\theta_i(\cos\theta_i - \omega). \tag{2.5}$$

Such a periodic solution may properly be called a discrete breather if it is spatially localized, that is, $\lim_{i\to\pm\infty} \theta_i = 0$.

In section 3 we shall prove the existence of discrete breathers for $\alpha$ sufficiently small and in section 4 we shall study them numerically for a range of values of $\alpha$.

Note that for all $\alpha$ there is a set of static solutions in which each spin can independently be chosen to point either up or down, since in each case we have that $\sin\theta_i = 0$ for all $i$, which clearly solves equation (2.5). These solutions will play an important role later in our discussion.

Finally, in this section, we address the continuum limit $\alpha \to \infty$. Write $\alpha = 1/h^2$ and regard $\boldsymbol{n}_i$ as the value of a continuous function $\boldsymbol{n}(x)$ sampled at the lattice points $x = \mathrm{i}h$. Taking the continuum limit $h \to 0$, the Hamiltonian (2.1) becomes

$$H = \int \{\tfrac{1}{2}\boldsymbol{n}' \cdot \boldsymbol{n}' + \tfrac{1}{2}[1 - (\boldsymbol{n}_i \cdot \boldsymbol{e}_3)^2]\}\,\mathrm{d}x \tag{2.6}$$

and the equation of motion is

$$\dot{\boldsymbol{n}} = \boldsymbol{n} \times \boldsymbol{n}'' + (\boldsymbol{n} \cdot \boldsymbol{e}_3)(\boldsymbol{n} \times \boldsymbol{e}_3) \tag{2.7}$$

where prime denotes differentiation with respect to $x$.

This partial differential equation has time periodic, exponentially localized solutions known as magnetic solitons [11]. At this point it is perhaps worth pointing out that there is an unfortunate difference in nomenclature, in that in the discrete case time periodic localized solutions are known as breathers, whereas in the continuum model they are termed solitons.

We shall continue to use the term soliton when referring to the continuum limit, but the reader should be aware that it has exactly the same time dependence as the discrete breather and moreover, as we shall see later, the soliton can be obtained from the discrete breather in the continuum limit.

Using the same form for the time dependence as in the discrete case (2.4), i.e.

$$\boldsymbol{n}(x,t) = (\sin\theta(x)\cos\omega t, -\sin\theta(x)\sin\omega t, \cos\theta(x)) \tag{2.8}$$

equation (2.7) yields the second-order ordinary differential equation

$$\theta'' = (\cos\theta - \omega)\sin\theta \tag{2.9}$$

which, of course, is also obtained from the continuum limit of (2.5). The boundary conditions for a soliton solution, located at the origin, are $\theta'(0) = \theta(\infty) = 0$. Equation (2.9) can be integrated explicitly and the solution satisfying the correct boundary conditions is given by

$$\theta(x) = \cos^{-1}\left\{\frac{2\omega}{1-(1-\omega)\tanh^2\left(x\sqrt{1-\omega}\right)} - 1\right\}. \tag{2.10}$$

Since we require the soliton to be a smooth exponentially localized solution, this formula shows that the frequency must be restricted to the range $\omega \in (0, 1)$. There is a second type of soliton solution [11] for which $\omega < 0$, but this has a different structure from (2.10); in particular $\boldsymbol{n} = -\boldsymbol{e}_3$ at the centre of the soliton for all $\omega$. This negative-frequency soliton will not arise in our discussion, so in this paper when we refer to a soliton we shall mean the solution (2.10).

## 3. Analytic results on discrete breathers

Following the 'homoclinic orbit' approach of Flach [7], one would like to prove directly the existence of solutions of (2.5) with the correct boundary behaviour, using techniques of dynamical systems theory. Unfortunately, equation (2.5) does not determine a well defined homeomorphism of the torus, $(\theta_{i-1}, \theta_i) \mapsto (\theta_i, \theta_{i+1})$, so the direct approach is not convenient here.

However, we may still prove the existence of breathers in this system by continuation of one-site breathers from the decoupled limit ($\alpha = 0$), in the manner of Aubry and MacKay's work on oscillator networks [13]. Here we have an algebraic system rather than an infinite system of ODEs so the details are considerably less technical (compare, for example, with [9]), and will be treated with corresponding brevity. The idea is that when $\alpha = 0, \omega \in (-1, 1)$, (2.5) supports the almost trivial solution

$$\theta_i^b = \begin{cases} 0 & i \neq 0 \\ \cos^{-1}\omega & i = 0 \end{cases} \tag{3.1}$$

in which every spin remains pointing up except one (whose location we have chosen to be $i = 0$), which precesses with frequency $\omega$ around a circle of fixed latitude. Note that there is no reason to assume that $\omega > 0$ as we had to in the continuum system. Keeping $\omega$ fixed, the existence of breathers for all $\alpha$ sufficiently small will follow from an implicit function theorem argument.

To be precise, let $F : \ell_2 \oplus \mathbb{R} \to \ell_2$ such that

$$\begin{aligned}[F(\theta,\alpha)]_i = {} & (\cos\theta_i - \omega)\sin\theta_i - \alpha[\cos\theta_i(\sin\theta_{i+1} + \sin\theta_{i-1}) \\ & - \sin\theta_i(\cos\theta_{i+1} + \cos\theta_{i-1})]\end{aligned} \tag{3.2}$$

where $\ell_2$ is the Banach space of sequences $\theta : \mathbb{Z} \to \mathbb{R}$ with finite norm

$$\|\theta\|_{\ell_2} = \left[\sum_i \theta_i^2\right]^{\frac{1}{2}}. \tag{3.3}$$

Note that $\theta \in \ell_2$ is a solution of (2.5) at coupling $\alpha$ if and only if $F(\theta, \alpha) = 0$. Note also that every $\theta \in \ell_2$ converges to 0 as $i \to \pm\infty$, so such a zero of $F(\cdot, \alpha)$ is a discrete breather. For all $\omega \in (-1, 1)$, $F(\theta^b, 0) = 0$, where $\theta^b$ is the one-site breather defined in (3.1), and the partial differential of $F$ with respect to the $\ell_2$ factor at $(\theta, \alpha) = (\theta^b, 0)$ is easily seen to be an isomorphism $DF_{(\theta^b,0)} : \ell_2 \to \ell_2$, that is, a bijection with bounded inverse. In fact this linear map is diagonal:

$$[DF_{(\theta^b,0)}\,\delta\theta]_i = \begin{cases} (1-\omega)\delta\theta_i & i \neq 0 \\ -(1-\omega^2)\delta\theta_0 & i = 0. \end{cases} \tag{3.4}$$

Hence we may apply the implicit function theorem [4] to obtain the following

**Theorem 1.** *For all $\omega \in (-1, 1)$ there exist $\epsilon > 0$ and a $C^1$ map $[0, \epsilon) \to \ell_2$, denoted $\alpha \mapsto \theta^\alpha$, such that $\theta^\alpha$ is a frequency $\omega$, coupling $\alpha$ solution of (2.5) and $\theta^0 = \theta^b$. The map $\alpha \mapsto \theta^\alpha$ is unique provided $\epsilon$ is chosen sufficiently small.*

As noted above, since the continuation occurs in $\ell_2$, it has weak spatial localization built in. This can be improved to exponential spatial localization (that is, there exist $C, \lambda > 1$ such that $|\theta_i| < C\lambda^{-|i|}$) by applying some standard results of Baesens and MacKay. The idea is to differentiate the continuation equation $F(\theta^\alpha, \alpha) = 0$ with respect to $\alpha$ to obtain an ODE on $\ell_2$, namely,

$$\frac{\mathrm{d}\theta^\alpha}{\mathrm{d}\alpha} = [DF_{(\theta^\alpha,\alpha)}]^{-1}\Delta(\theta^\alpha) \tag{3.5}$$

where $\Delta : \ell_2 \to \ell_2$ such that

$$[\Delta(\theta)]_i = \cos\theta_i(\sin\theta_{i+1} + \sin\theta_{i-1}) - \sin\theta_i(\cos\theta_{i+1} + \cos\theta_{i-1}). \tag{3.6}$$

The theorem above may be interpreted as asserting the local existence and uniqueness of a solution to the initial-value problem $\theta^0 = \theta^b$ for (3.5). Now $\Delta(\theta^\alpha)$ is clearly exponentially localized provided $\theta^\alpha$ is, as is $[DF_{(\theta^\alpha,\alpha)}]^{-1}\Delta(\theta^\alpha)$ by theorem 3 of [3]. Thus one obtains an exponential decay estimate for $\mathrm{d}\theta^\alpha/\mathrm{d}\alpha$ at $\alpha_0$ given a decay estimate for $\theta^{\alpha_0}$. This may be integrated to show that the estimate for $\theta^{\alpha_0}$, if chosen correctly, remains valid in a finite interval containing $\alpha_0$ (see the proof of theorem 2 of [3], for example). It remains then to note that the initial datum $\theta^b$ trivially satisfies *all* exponential decay criteria (i.e. one can choose any $\lambda > 1$), so exponential localization persists for $\alpha$ sufficiently small.

We may deduce the optimal exponent $\lambda$ for given $\omega$ and $\alpha$ by linearizing equation (2.5) about $\theta = 0$:

$$\delta\theta_{i+1} - \left[2 + \frac{1-\omega}{\alpha}\right]\delta\theta_i + \delta\theta_{i-1} = 0. \tag{3.7}$$

The general solution to (3.7) is $\delta\theta_i = A\lambda^i + B\lambda^{-i}$ where

$$\lambda = 1 + \frac{1-\omega}{2\alpha} + \left[\frac{1-\omega}{\alpha} + \left(\frac{1-\omega}{2\alpha}\right)^2\right]^{\frac{1}{2}}. \tag{3.8}$$

It is this type of exponential decay, $|\theta_i| \sim \lambda^{-|i|}$, which we shall encounter in our numerical analysis.

Another interesting piece of information can be deduced from equation (3.5), namely the tangent vector to the continuation curve in $\ell_2$, that is, the direction of continuation away from $\alpha = 0$. Substituting (3.1) and (3.4) into (3.5) at $\alpha = 0$ yields

$$\left[\left.\frac{\mathrm{d}\theta^\alpha}{\mathrm{d}\alpha}\right|_{\alpha=0}\right]_i = \begin{cases} 0 & |i| > 1 \\ \dfrac{1+\omega}{\sqrt{1-\omega^2}} & |i| = 1 \\ \dfrac{2}{\sqrt{1-\omega^2}} & i = 0. \end{cases} \tag{3.9}$$

So the continuation initially proceeds by pulling the central spin, $\boldsymbol{n}_0$, further away from the vacuum $\boldsymbol{e}_3$, and pulling its nearest neighbours, $\boldsymbol{n}_{\pm 1}$ away from $\boldsymbol{e}_3$ in the same direction (as $\boldsymbol{n}_0$ and each other), while leaving all other spins fixed at $\boldsymbol{e}_3$, to first order.

We have proved the existence of a continuation of the one-site breather $\theta^b$, but the same argument can be applied to any zero of $F(\cdot, 0) : \ell_2 \to \ell_2$ to prove the existence of more general discrete breathers at small $\alpha$. Clearly, if $F(\theta, 0) = 0$ then $\theta_i \in \pi\mathbb{Z} \cup \cos^{-1}\{\omega\}$ for all $i$, and given that $\theta \in \ell_2$, $\theta_i = 0$ for all $|i|$ sufficiently large. So one can construct frequency $\omega$ solutions at $\alpha = 0$ like

$$\tilde{\theta} = (\ldots, 0, 0, \cos^{-1}\omega, \pi, \pi, \pi, \cos^{-1}\omega, 0, 0, \ldots) \tag{3.10}$$

for example. It is easy to check that $DF_{(\tilde{\theta},0)}$ is an isomorphism, so an analogous result to the theorem above applies here also. Of particular relevance to the numerical work in section 4 will be those periodic solutions obtained by continuing $\alpha = 0$ solutions with even reflection symmetry about $i = 0$, that is, $\theta_{-i} \equiv \theta_i$. Such a solution may be specified by a finite coding sequence [14] representing the values of $\theta_i$ for $i = 0, 1, 2, \ldots$ by + if $\theta_i = 0$, $o$ if $\theta_i = \cos^{-1}\omega$ and $-$ if $\theta_i = \pi$, with the convention that the last symbol represents the constant tail of the sequence. Of course, since $\theta \in \ell_2$, each coding sequence must end in +, so the last symbol is redundant. Nevertheless, we include it in order to make the notation more suggestive. The symbols themselves are meant to represent the directions of the central spins: up is +, down $-$, while $o$ is somewhere ($\omega$ dependent) in between. We shall refer to those breathers obtained by continuing such a solution by the same coding sequence. Hence $\theta^\alpha$, the continuation of $\theta^b$ is a ($o$+)-breather, while $\tilde{\theta}$ and its continuation are ($--o$+)-breathers, for example.

## 4. Numerical results on discrete breathers

In this section we present the results of an extensive numerical investigation of the continuation of one-site and various multi-site breathers from the anti-continuum limit. To construct numerical solutions we must first truncate to a finite number of lattice sites, which we implement by fixing vacuum boundary conditions, $\theta_i = 0$ for $i = \pm N$, and restricting to the interior of the lattice $|i| < N$. Furthermore, the solutions we consider are symmetric about the central lattice site, that is, $\theta_i = \theta_{-i}$, so only the sites $i \geqslant 0$ need be considered, with an appropriate modification at the central site $i = 0$. Explicitly, the task of finding a numerical solution reduces to finding a zero of the following $(N + 1)$-component vector:

$$F_i = \begin{cases} \alpha[\cos\theta_i(\sin\theta_{i+1} + \sin\theta_{i-1}) - \sin\theta_i(\cos\theta_{i+1} + \cos\theta_{i-1})] + \sin\theta_i(\omega - \cos\theta_i) \\ 0 < i < N \\ 2\alpha[\cos\theta_0 \sin\theta_1 - \sin\theta_0 \cos\theta_1] + \sin\theta_0(\omega - \cos\theta_0) \\ i = 0 \\ \theta_N \\ i = N \end{cases} \tag{4.1}$$

as a function of the $(N + 1)$ values $\theta_i$, $i = 0, \ldots, N$.

To find a zero of the vector $F_i$, for a given value of $\alpha$, we begin with the value $\alpha = 0$, where we have the explicit solution corresponding to the trivial one-site breather (3.1) (and later we use other multi-site breathers). We then increase $\alpha$ by a small amount and use a Newton–Raphson scheme to converge to the new solution. This process is repeated until the desired value of $\alpha$ has been obtained. During the calculation the determinant of the Jacobian matrix $J_{ij} = \partial F_i / \partial \theta_j$ is monitored to ensure that it is non-zero, as a check that the scheme is not accidentally jumping to a different solution branch. The results presented below were

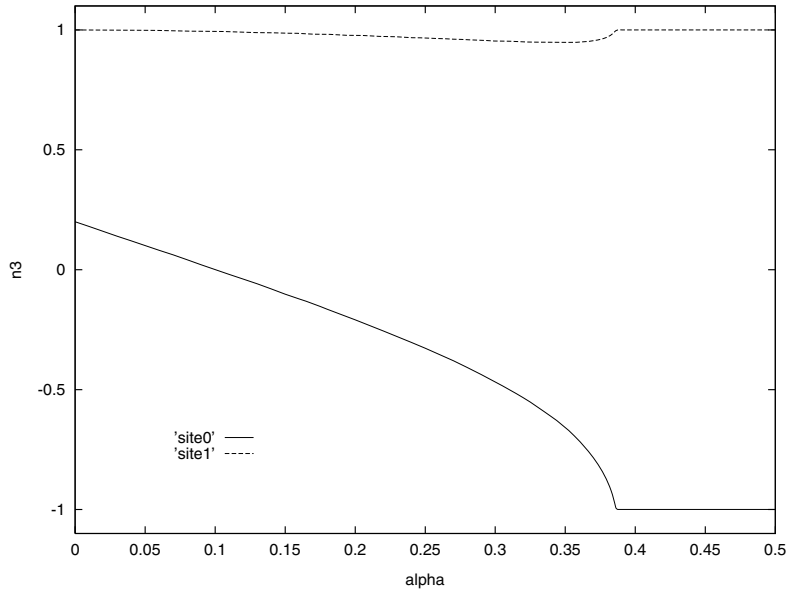


**Figure 1.** Plots of $\cos\theta_0$ and $\cos\theta_1$ for the continuation of the $(o+)$-breather with $\omega = 0.2$, from $\alpha = 0$ to 0.5.

obtained from the value $N = 20$, though different size lattices were checked to confirm that, providing $N$ is sufficiently large, the results are not sensitive to the number of sites.

In figure 1 we display the results of the continuation of the $(o+)$-breather, with frequency $\omega = 0.2$, from $\alpha = 0$ to 0.5. Presented are plots of $\cos\theta_0$ and $\cos\theta_1$, that is, the third component of the spin for the central and next to central sites. From this plot it is clear that the $(o+)$-breather continues until it joins the static $(-+)$ solution. This is true for all frequencies in the band $\omega \in (-1, 0.424]$, where we have computed the edge of the band to within the numerical accuracy given. It is not surprising that for $\omega$ close to $-1$ the $(o+)$-breather continues to the static $(-+)$ solution since for $\alpha = 0$ the $(o+)$-breather tends to the $(-+)$ solution as $\omega \to -1$.

In figure 2 we present the results of a similar calculation, but this time the initial $(o+)$-breather has a frequency $\omega = 0.5$. The values of $\cos\theta_0$ and $\cos\theta_1$ are shown as solid curves and the dashed curves represent the same quantities for the continuum soliton solution (2.10) sampled at lattice sites $x = 0$ and $h$, where $h = 1/\sqrt{\alpha}$. As the coupling $\alpha$ is increased, the values at these sites tend towards those of the continuum soliton solution, demonstrating that the $(o+)$-breather approaches the soliton solution in the continuum limit. As further evidence, in figure 3 we plot $\cos\theta_i$ for all lattice sites, for the value $\alpha = 2$, superimposed with the soliton solution given in (2.10), with $x = \mathrm{i}/\sqrt{2}$. As a final check, starting with initial conditions obtained from sampling the soliton solution at the lattice sites and continuing backwards to $\alpha = 0$, we find that we recover the $(o+)$-breather. We have also verified that the decay rate of the $(o+)$-breather shown in figure 3 fits extremely well to the derived exponential decay constant given in (3.8).

Similar results apply for all frequencies in the band $\omega \in (0.424, 1)$, with the $(o+)$-breather continuing to the soliton solution, although the region in which $\omega$ is close to unity is numerically inaccessible within the present scheme since the soliton has a relatively slow spatial decay in this region.

Just below the interface of the two bands, that is for $0 \leqslant 0.424 - \omega \ll 1$, there is a more complicated bifurcation structure between the $(o+)$-breather and the static $(-+)$ solution than

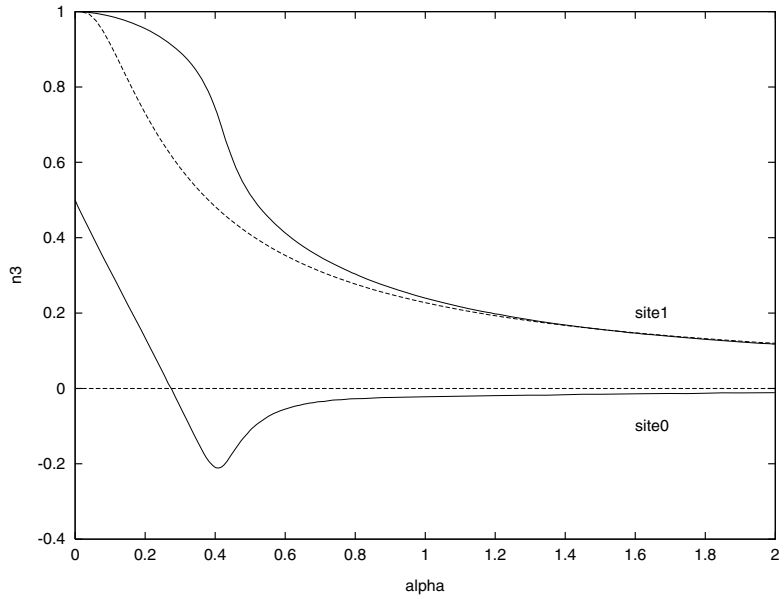


**Figure 2.** Plots of $\cos\theta_0$ and $\cos\theta_1$ for the continuation of the ($o$+)-breather (solid curves) with $\omega = 0.5$, from $\alpha = 0$ to 2. The dashed curves are the corresponding quantities for the soliton solution.

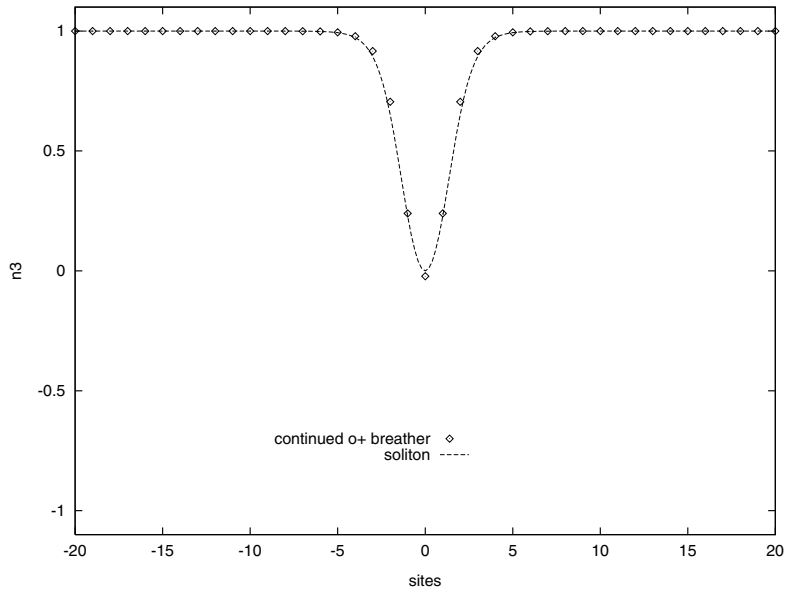


**Figure 3.** $\cos\theta_i$ for all the lattice sites of the $\omega = 0.5$ ($o$+)-breather with $\alpha = 2$ (diamonds). The dashed curve is the corresponding soliton solution.

in the bulk of the lower band $(-1, 0.424]$. To examine this region requires a slightly more sophisticated numerical approach, as we now describe, by illustrating the case $\omega = 0.42$.

For $\omega = 0.42$ the continuation of the ($o$+)-breather is presented in figure 4, where the dashed curve represents the value of $\cos\theta_0$. The continuation fails at $\alpha = \alpha^* = 0.4085$,

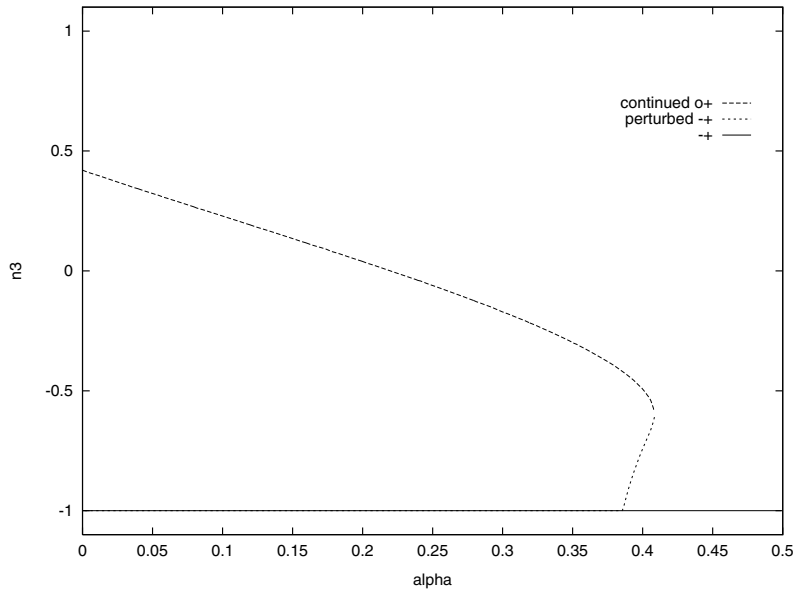


**Figure 4.** $\cos\theta_0$ for the continuation of the $(o+)$-breather (dashed curve), the static $(-+)$-solution (solid line), and the perturbed $(-+)$-solution (dotted curve).

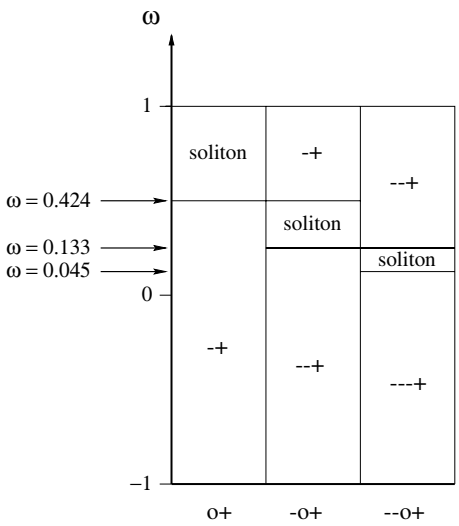


**Figure 5.** A table displaying the results, as $\omega$ is varied, of continuing breathers of type $(o+)$, $(-o+)$ and $(--o+)$. The symbol at the foot of each column indicates which breather is being continued and the symbol inside the column represents the end result of the continuation at that frequency.

where the determinant of the Jacobian matrix $J$ is zero. We expect that this solution still bifurcates from the static $(-+)$ solution, but that it first turns around in $\alpha$ space. To confirm this expectation we need to find the value $\alpha = \widehat{\alpha}$, at which the bifurcation of the $(-+)$ solution takes place, and compute the tangent vector in the direction of this bifurcation. The Jacobian

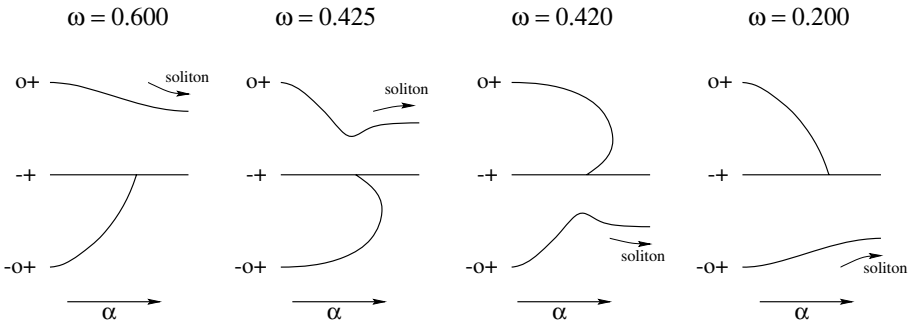


**Figure 6.** A schematic diagram to indicate how the bifurcation pattern between the $(-+)$ solution and the $(o+)$ and $(-o+)$ breathers varies with $\omega$.

of the $(-+)$ solution is the tridiagonal matrix

$$J = \begin{pmatrix} 2\alpha-\omega-1 & -2\alpha & & & & \\ -\alpha & \omega-1 & \alpha & & & \\ & \alpha & -2\alpha+\omega-1 & \alpha & & \\ & & \cdots & \cdots & \cdots & \\ & & & \alpha & -2\alpha+\omega-1 & \alpha \\ & & & & 0 & 1 \end{pmatrix}. \tag{4.2}$$

Computing the determinant of this matrix (for $N = 20$) and setting $\omega = 0.42$, we find that $\det J$ has only one real and positive root, which occurs at $\alpha = \widehat{\alpha} = 0.3858$. Note that this calculation provides the first check on our bifurcation assumption since we require that $\widehat{\alpha} < \alpha^*$, which is indeed true. Substituting $\alpha = \widehat{\alpha}$ into $J$ we then compute the eigenvector, $\delta\theta$, corresponding to the zero eigenvalue, normalized so that its norm $|\delta\theta|^2 = \epsilon \ll 1$. Finally, we take the $(-+)$ solution, in which $\theta_0 = \pi$ and $\theta_i = 0$ for $i > 0$, and add the perturbation $\delta\theta$, to create an initial condition which we then iterate to converge to a solution for a value of $\alpha$ obtained by incrementing $\widehat{\alpha}$ by a small amount. Following this solution for increasing $\alpha$ we find that it continues until $\alpha = \alpha^*$, where it meets the end point of the continued $(o+)$-breather. This is illustrated in figure 4, where we plot $\cos\theta_0$ (dotted curve) for the solution branch obtained by perturbation of the static $(-+)$ solution, as just described. Following the end point of this solution branch backwards in $\alpha$ confirms that it joins the static $(-+)$ solution at $\alpha = \widehat{\alpha}$.

To summarize, the results of the continuation of the $(o+)$-breather, as $\omega$ is varied, are represented in the first column of figure 5, and presented schematically in the upper half of figure 6. For $\omega \in (0.424, 1)$ the $(o+)$-breather continues to the soliton, for $\omega$ outside this range, but close to 0.424, it turns back and joins the static $(-+)$ solution, and in the bulk of the band $(-1, 0.424]$ it joins the static $(-+)$ solution without turning back.

For $\omega$ above 0.424 there is no longer a bifurcation of the static $(-+)$ solution with the $(o+)$-breather, but to fill in the full bifurcation pattern of the $(-+)$ solution we must now consider the continuation of the $(-o+)$-breather. Note that now the start point of the continuation, $\alpha = 0$, is already a multi-site breather, since we have applied reflection symmetric conditions, $\theta_i = \theta_{-i}$, and the breathing site is not located at $i = 0$.

In figure 7 we plot $\cos\theta_i$ for the first three sites, $i = 0, 1, 2$, for the continuation of the $(-o+)$-breather with frequency $\omega = -0.2$. Clearly, for this frequency, the $(-o+)$-breather continues to the static $(--+)$ solution, and this is true for all $\omega \in (-1, 0.133)$. From a similar earlier discussion, it follows that this result is to be expected, at least for $\omega$ near $-1$. For $\omega \in [0.133, 0.424]$ the $(-o+)$-breather approaches the soliton solution in the continuum limit.

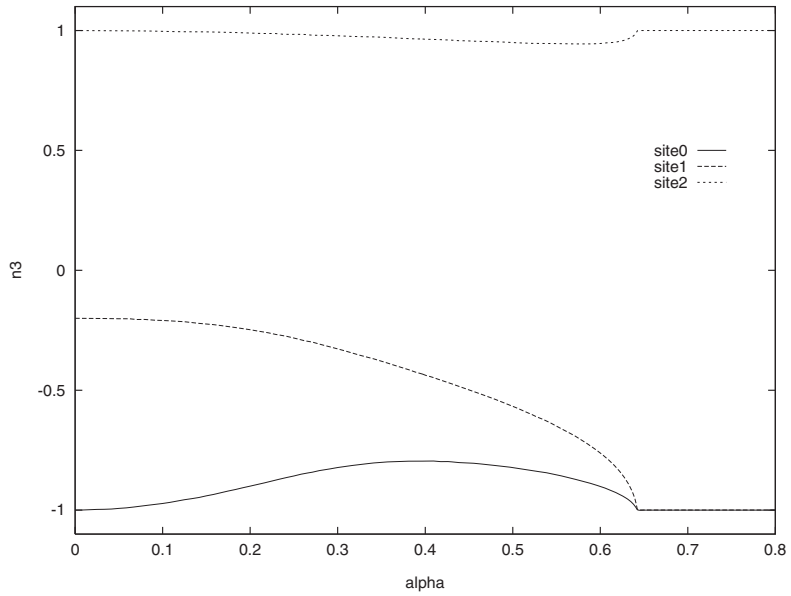


**Figure 7.** $\cos\theta_0, \cos\theta_1, \cos\theta_2$ for the continuation of the $\omega = -0.2$ $(-o+)$-breather for $\alpha \in [0, 0.8]$.

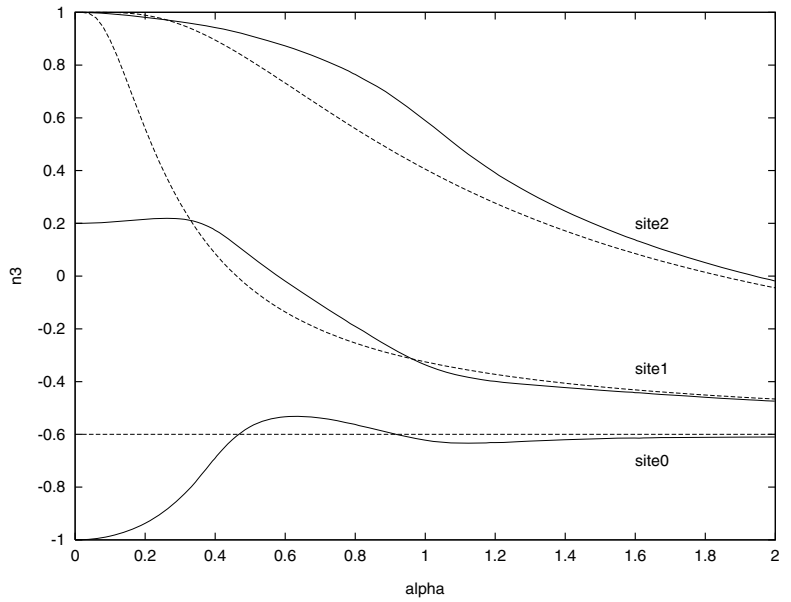


**Figure 8.** $\cos\theta_0, \cos\theta_1, \cos\theta_2$ (solid curves) for the continuation of the $\omega = 0.2$ $(-o+)$-breather for $\alpha \in [0, 2]$. The dashed curves are the corresponding quantities for the soliton solution.

As an example, for $\omega = 0.2$, we present in figure 8 a plot of $\cos\theta_i$ for the first three sites (solid curves) and also the corresponding quantities for the sampled soliton solution (dashed curves). For $\omega \in (0.424, 1)$ the $(-o+)$-breather continues to the static $(-+)$ solution, as demonstrated in figure 9 for $\omega = 0.55$. These results are summarized in the second column of figure 5.

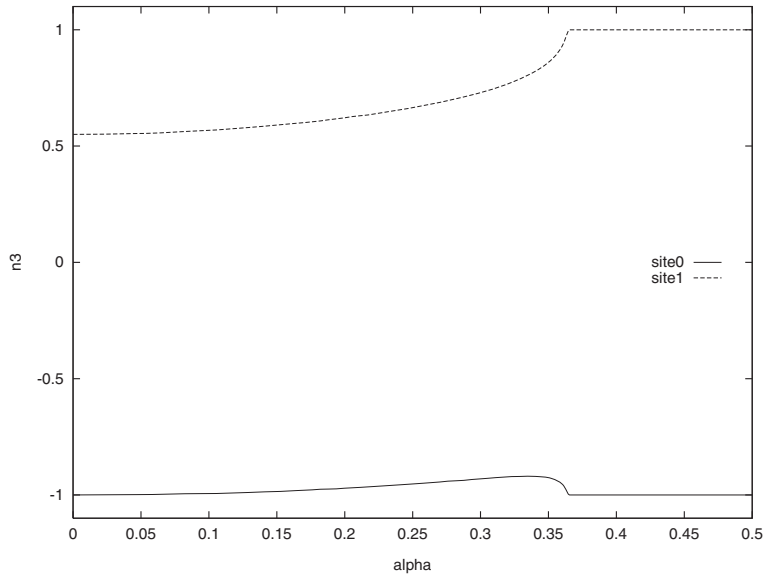


**Figure 9.** $\cos\theta_0$, $\cos\theta_1$ for the continuation of the $\omega = 0.55$ $(-o+)$-breather for $\alpha \in [0, 0.5]$.

It is, of course, no accident that the frequency ($\omega = 0.424$) at which the $(o+)$-breather fails to continue to the soliton is precisely that at which the $(-o+)$-breather begins to continue to the soliton. This can be understood by completing the bifurcation pattern of the $(-+)$ solution, using the above results on the continuation of the $(-o+)$-breather, to fill in the bottom half of the schematic diagram in figure 6. As presented in the diagram, there is always a bifurcation of the $(-+)$ solution, but it switches over from the $(-o+)$-breather to the $(o+)$-breather as the frequency is decreased to the critical value $\omega = 0.424$. At this point the $(o+)$-breather no longer continues to the soliton, but the $(-o+)$-breather now does. We have verified this structure with a number of detailed further calculations; for example, we have confirmed the turning back of the continuation of the $(-o+)$-breather by perturbing the $(-+)$ solution as described earlier.

The lower edge of the band $\omega \in [0.133, 0.424]$ can also be understood in a similar fashion by an analysis of the bifurcation pattern of the $(--+)$ solution, which requires computations of the continuation of the $(--o+)$-breather. These calculations have been performed and the results are summarized in the third column of figure 5. Again there is a soliton band, which begins at the frequency $\omega = 0.045$, and ends at the start of the $(-o+)$-breather soliton band where $\omega = 0.133$. Below the soliton band the $(--o+)$-breather continues to the $(---+)$ solution and above the soliton band it continues to the $(--+)$ solution. Computations confirm that the bifurcation pattern of the $(--+)$ solution is analogous to that of the $(-+)$ solution depicted in figure 6, with an extra $-$ sign inserted into the coding sequence of each solution together with a shift in the frequencies.

Given the above results we are naturally led to the conjecture that the pattern of soliton bands continues, with each band covering a smaller range of frequencies, but such that for any frequency $\omega \in (0, 1)$ there is a discrete breather solution whose continuation from $\alpha = 0$ tends to the soliton solution in the continuum limit $\alpha \to \infty$.

Generally, as mentioned in the introduction, discrete breathers in networks of coupled oscillators fail to continue beyond a certain coupling due to resonance with phonons.

In the system considered here, the role of phonons is played by spin waves,

$$\delta \boldsymbol{n}_i(t) = \begin{pmatrix} \cos(ki - \omega_p t) \\ \sin(ki - \omega_p t) \\ 0 \end{pmatrix} \tag{4.3}$$

which are travelling wave solutions of (2.3) linearized about the vacuum $\boldsymbol{n} = \boldsymbol{e}_3$. These have dispersion relation

$$\omega_p = 1 + 4\alpha \sin^2(k/2) \tag{4.4}$$

so the spin waves form a frequency band with $\omega_p \in [1, 1 + 4\alpha]$. Note that the maximal frequency spin wave ($k = \pi$) is standing, hence of the form (2.4) with frequency $\omega_p = 1+4\alpha$. It may equally well be regarded as periodic of frequency $\omega_p/n$ for any $n \in \mathbb{Z}^+$. Mathematically, a bifurcation in the continuation of breathers may only occur where $DF$ acquires nontrivial kernel, that is the equation of 'motion' (2.5) linearized about the breather supports a nonzero solution. Of course phonons, being linearized solutions about the *vacuum*, never lie in ker $DF$ strictly speaking. Nevertheless, since the breather approaches the vacuum exponentially fast as $|i| \to \infty$, it is generally accepted that the existence of a standing phonon of frequency $\omega_p = n\omega$ generically implies nontriviality of ker $DF$, that is, the phonon is close to a tangent vector in ker $DF$, approaching it asymptotically as $|i| \to \infty$. In the present case, the standing spin wave lies outside $\ell_2$, so cannot be close to ker $DF$, and hence cannot cause a bifurcation. In practice this technical point is irrelevant: the numerics are performed on a finite chain where such distinctions are impossible to make. Why then do the standing spin waves cause no bifurcations in the numerical continuation? The reason is that our map $F$ contains explicit parametric dependence on $\omega$, so only the standing spin wave of frequency $\omega_p = \omega$ is in the kernel of $DF$ at the vacuum. Higher harmonics, $\omega_p = n\omega$ are *not* linearized solutions of our ansatz-derived equation (2.5), and so cannot cause bifurcations. This is entirely consistent with physical intuition. These breathers, like those in the DNLS system, are monochromatic: their time dependence contains no higher harmonics so one does not expect them to resonate with the spin waves. It is precisely the imposition of a monochromatic ansatz (2.4) which introduced the parametric $\omega$ dependence discussed above.

## 5. Linear stability

Linear stability of breathers in networks of anharmonic oscillators was studied by Aubry in [1]. Despite the many superficial differences between spin chains and oscillator networks, we shall find that the analytic framework developed by Aubry readily adapts to this new setting, yielding similar results. In particular, we shall prove that ($o$+)-breathers of all frequencies $\omega \in (-1, 0) \cup (0, 1)$ must be linearly stable for sufficiently small $\alpha$ provided $\omega^{-1} \notin \mathbb{Z}$. Just how small $\alpha$ must be, and the stability properties of the various other breather types will be investigated numerically.

As in [1], it is technically convenient to truncate the lattice to (large but) finite size $N$ (the results will be independent of $N$). Existence of discrete breathers in such a system follows from an identical argument to that of theorem 1, but with $\ell_2$ replaced by $\mathbb{R}^N$ with its usual norm. Equation (2.3) along with fixed endpoints $\boldsymbol{n}_0 = \boldsymbol{n}_{N+1} = 0$ then define a flow on phase space $M = (S^2)^N$. Crucial to the analysis is the fact that this flow is Hamiltonian with respect to the natural symplectic structure on $M$, namely

$$\Omega = \sum_i \Omega_i \tag{5.1}$$

where $\Omega_i$ is the area form on the $i$th 2-sphere. The Hamiltonian $H : M \to \mathbb{R}$ is the truncation of (2.1), again with fixed endpoints. It follows that the flow is symplectomorphic.

A period $T$ solution of the system is a fixed point of the return map $P_T : M \to M$, $P_T : n(0) \mapsto n(T)$. Such a solution is said to be linearly stable if the spectrum of its associated Floquet map $\mathcal{F}\ell = (\mathrm{d}P_T)_{n(0)} : T_{n(0)}M \to T_{n(T)=n(0)}M$ lies within the closed unit disc $D = \{z \in \mathbb{C} : |z| \leqslant 1\}$. Recall that $\mathcal{F}\ell : \delta n(0) \mapsto \delta n(T)$ where $\delta n(t)$ is the solution of the linearization of (2.3) about the solution $n(t)$, explicitly,

$$\delta\dot{\boldsymbol{n}}_i = \alpha[\boldsymbol{n}_i \times (\delta\boldsymbol{n}_{i+1} + \delta\boldsymbol{n}_{i-1}) + \delta\boldsymbol{n}_i \times (\boldsymbol{n}_{i+1} + \boldsymbol{n}_{i-1})] + (\delta\boldsymbol{n}_i \cdot \boldsymbol{e}_3)\boldsymbol{n}_i \times \boldsymbol{e}_3. \tag{5.2}$$

Since $P_T$ is a symplectomorphism, $\mathcal{F}\ell$ is a symplectic map, that is

$$\Omega(\mathcal{F}\ell\,\delta n, \mathcal{F}\ell\,\delta n') \equiv \Omega(\delta n, \delta n'). \tag{5.3}$$

It follows that if $\lambda \in \operatorname{spec}\mathcal{F}\ell$, so are $\bar{\lambda}$, $1/\lambda$ and $1/\bar{\lambda}$. Hence the solution is linearly stable if and only if $\operatorname{spec}\mathcal{F}\ell$ lies on the unit circle $\partial D = \{z \in \mathbb{C} : |z| = 1\}$.

It is straightforward to construct $\mathcal{F}\ell$ explicitly for all the breathers considered in sections 3 and 4 in the uncoupled limit, $\alpha = 0$. For each $\boldsymbol{n}_i(0) = (\sin\theta_i, 0, \cos\theta_i)$ define the ordered orthonormal basis

$$(\boldsymbol{\varepsilon}_i = (\cos\theta_i, 0, \sin\theta_i), \boldsymbol{e}_2) \tag{5.4}$$

for $T_{\boldsymbol{n}_i(0)}S^2$, so that $T_{n(0)}M = \bigoplus_i \operatorname{span}\langle\boldsymbol{\varepsilon}_i, \boldsymbol{e}_2\rangle$. Relative to this basis, the symplectic form has the usual block matrix expression, namely

$$\Omega = \operatorname{diag}\left(\ldots, R\left(\frac{\pi}{2}\right), R\left(\frac{\pi}{2}\right), \ldots\right) \tag{5.5}$$

where $R(\psi)$ is the $SO(2)$ matrix which performs a clockwise rotation through angle $\psi$, explicitly,

$$R(\psi) = \begin{pmatrix} \cos\psi & \sin\psi \\ -\sin\psi & \cos\psi \end{pmatrix}. \tag{5.6}$$

The Floquet matrix of the frequency $\omega$ $(o+)$-breather is

$$\mathcal{F}\ell = \operatorname{diag}(\ldots, R(T), R(T), S, R(T), R(T), \ldots) \tag{5.7}$$

where $T = 2\pi/\omega$ and $S$ is the matrix

$$S = \begin{pmatrix} 1 & 0 \\ (1-\omega^2)T & 1 \end{pmatrix}. \tag{5.8}$$

Similarly, the $(-o+)$-breather has Floquet matrix

$$\mathcal{F}\ell = \operatorname{diag}(\ldots, R(T), R(T), S, R(T), S, R(T), R(T), \ldots) \tag{5.9}$$

and so on. Clearly all these matrices have $\operatorname{spec}\mathcal{F}\ell = \{\mathrm{e}^{\pm\mathrm{i}T}, 1\} \subset \partial D$ so the uncoupled breathers of all types are linearly stable.

As $\alpha$ increases from 0, theorem 1 guarantees the existence of a continuous family of symplectic maps $\mathcal{F}\ell_\alpha$ (recall that $\alpha \mapsto \theta_\alpha$ is $C^1$) whose eigenvalues depend continuously on $\alpha$. Do these eigenvalues remain on $\partial D$? Clearly only coincident pairs may leave $\partial D$ in tandem, by the symmetry properties of $\operatorname{spec}\mathcal{F}\ell$. Krein theory [1] states that an eigenvalue $\lambda \in \partial D$ may bifurcate off the unit circle only if its associated Krein signature is indefinite. This signature is defined as follows. Let $E_\lambda \subset \mathbb{C}^{2N}$ be the $\lambda$ eigenspace of $\mathcal{F}\ell$ and $V_\lambda := \operatorname{Re}(E_\lambda \oplus E_{1/\lambda}) \subset \mathbb{R}^{2N}$. Then on $V_\lambda$ one defines a bilinear form $Q_\lambda : V_\lambda \oplus V_\lambda \to \mathbb{R}$ such that

$$Q_\lambda(\xi, \eta) := \Omega(\xi, \mathcal{F}\ell\,\eta). \tag{5.10}$$

The Krein signature of $\lambda$ is the signature of this bilinear form. Hence, $\lambda$ may bifurcate off $\partial D$ only if $Q_\lambda$ is indefinite, that is, the diagonal map $\xi \mapsto Q_\lambda(\xi, \xi)$ is neither positive definite nor negative definite on $V_\lambda \backslash \{0\}$.

Applying this theory to (5.7) one sees that $V_{e^{iT}} \equiv V_{e^{-iT}} \cong \mathbb{R}^{2N-2}$, $V_1 \cong \mathbb{R}^2$,

$$Q_{e^{iT}}(\xi,\xi) = -(\sin T)\,\xi^T\xi \qquad Q_1(\xi,\xi) = (1-\omega^2)\xi_1^2. \tag{5.11}$$

Provided $\sin T \neq 0$, i.e. $\omega^{-1} \notin \mathbb{Z}$, $Q_{e^{iT}}$ is definite and hence all the eigenvalues $e^{\pm iT}$ must remain on $\partial D$, at least for sufficiently small $\alpha$. On the other hand, $Q_1$ is only positive *semi*-definite, so no such constraint applies to the double eigenvalue $\lambda = 1$. Note however that for any nonstatic period $T$ solution $n(t)$ of an autonomous dynamical system, $\dot{n}(0)$ is an eigenvector of $\mathcal{F}\ell$ with $\mathcal{F}\ell\,\dot{n}(0) = \dot{n}(0)$ by time translation invariance. It follows that one copy of the eigenvalue $\lambda = 1$ is fixed for all $\alpha$. The second is also fixed for sufficiently small $\alpha$ since to move it would have to (at least) double up due to the symmetry properties of spec $\mathcal{F}\ell$. Hence, we have proved:

**Theorem 2.** *For each $N \in \mathbb{Z}^+$ and for all $\omega \in (-1,1)\backslash\{0\}$ such that $\omega^{-1} \notin \mathbb{Z}$, there exists $\tilde{\alpha}(\omega) > 0$ such that for all $\alpha \in [0, \tilde{\alpha}(\omega))$ the continued $(o+)$-breathers, whose existence on the N site lattice is guaranteed by theorem 1, are linearly stable.*

Unfortunately, this argument cannot be applied to multisite breathers such as $(-o+)$. This is because $V_1$ is now (at least) four dimensional and $Q_1$ remains only semidefinite. Time translation symmetry is not sufficient to fix all four copies of $\lambda = 1$ under perturbation of $\alpha$, so while the $\alpha = 0$ $(-o+)$-, $(--o+)$- etc breathers are all stable, instability may develop for arbitrarily small $\alpha$. Note, however, that the Krein criterion is necessary but *not sufficient*: it does not guarantee instability of $\alpha > 0$ multisite breathers, nor of $(o+)$-breathers with $\omega^{-1} \in \mathbb{Z}$. To investigate these issues, we must resort once again to numerical analysis.

One may vastly simplify the task of numerically constructing the Floquet matrix $\mathcal{F}\ell$ for this problem by transforming to a co-rotating coordinate system. Let $\mathcal{R} : \mathbb{R} \to SO(3)$ such that

$$\mathcal{R}(t) = \mathrm{diag}\,(R(\omega t), 1) \tag{5.12}$$

where $R(t)$ is the the $SO(2)$ matrix defined in equation (5.6), and define new variables $\boldsymbol{u}_i(t)$ such that

$$\boldsymbol{n}_i(t) = \mathcal{R}(t)\boldsymbol{u}_i(t). \tag{5.13}$$

Then the equations of motion become

$$\dot{\boldsymbol{u}}_i = \alpha\boldsymbol{u}_i \times (\boldsymbol{u}_{i+1} + \boldsymbol{u}_{i-1}) + (\boldsymbol{u}_i \cdot \boldsymbol{e}_3)(\boldsymbol{u}_i \times \boldsymbol{e}_3) - \mathcal{A}\boldsymbol{u}_i \tag{5.14}$$

where $\mathcal{A} = (\mathcal{R}^{-1}\dot{\mathcal{R}})(t) \equiv (\mathcal{R}^{-1}\dot{\mathcal{R}})(0) \in so(3)$ is a constant antisymmetric matrix. The point is that all the breather solutions we have been considering are *static* in this coordinate system, namely $\boldsymbol{u}_i(t) = (\sin\theta_i, 0, \cos\theta_i)$, where $\theta_i$ satisfies (2.5) as before. Consequently, the linearized flow is defined by an *autonomous* linear system of ODEs,

$$\delta\dot{\boldsymbol{u}}_i = \alpha[\boldsymbol{u}_i \times (\delta\boldsymbol{u}_{i+1} + \delta\boldsymbol{u}_{i-1}) + \delta\boldsymbol{u}_i \times (\boldsymbol{u}_{i+1} + \boldsymbol{u}_{i-1})] + (\delta\boldsymbol{u}_i \cdot \boldsymbol{e}_3)\boldsymbol{u}_i \times \boldsymbol{e}_3 - \mathcal{A}\delta\boldsymbol{u}_i. \tag{5.15}$$

Using the basis $\{\boldsymbol{\varepsilon}_i, \boldsymbol{e}_2\}$ for $T_{\boldsymbol{u}_i}S^2$ and writing

$$\delta\boldsymbol{u}_i = a_i(t)\boldsymbol{\varepsilon}_i + b_i(t)\boldsymbol{e}_2 \tag{5.16}$$

this system reduces to

$$\begin{pmatrix}\dot{a}\\ \dot{b}\end{pmatrix} = \Lambda\begin{pmatrix}a\\ b\end{pmatrix} = \begin{pmatrix}0 & \Lambda^+\\ \Lambda^- & 0\end{pmatrix}\begin{pmatrix}a\\ b\end{pmatrix} \tag{5.17}$$

where $\Lambda^\pm$ are constant, tridiagonal, symmetric real $N \times N$ matrices with components

$$\begin{aligned}\Lambda^+_{ij}(\theta) &= \alpha\{-\delta_{i,j+1} - \delta_{i,j-1} + [\cos(\theta_i - \theta_{i+1}) + \cos(\theta_i - \theta_{i-1})]\delta_{i,j}\}\\ &\quad + \cos\theta_i(\cos\theta_i - \omega)\delta_{i,j}\\ \Lambda^-_{ij}(\theta) &= \alpha\{\cos(\theta_i - \theta_j)(\delta_{i,j+1} + \delta_{i,j-1}) - [\cos(\theta_i - \theta_{i+1}) + \cos(\theta_i - \theta_{i-1})]\delta_{i,j}\}\\ &\quad + (\omega\cos\theta_i - \cos 2\theta_i)\delta_{i,j}.\end{aligned} \tag{5.18}$$

The Floquet matrix $\mathcal{F}\ell : \delta\boldsymbol{n}(0) \mapsto \delta\boldsymbol{n}(T)$ is simply

$$\mathcal{F}\ell = \mathcal{R}(T)\exp(T\Lambda)\mathcal{R}(0)^{-1} \equiv \exp(T\Lambda). \tag{5.19}$$

One may easily check that equations (5.18), (5.19) reproduce the $\alpha = 0$ matrices previously obtained. Note that we have *not* imposed a monochromatic ansatz for the perturbation: $\delta\boldsymbol{u}_i$ and hence $\delta\boldsymbol{n}_i$ are permitted to have arbitrary time dependence. We have merely made a particularly convenient choice of coordinates.

So a period $T$ breather is linearly stable if and only if its corresponding $\Lambda$ matrix has spec $\Lambda \subset \mathrm{i}\mathbb{R} \subset \mathbb{C}$, a criterion which is trivial to test numerically. This should be contrasted with the procedure usually employed in numerical linear stability analyses, where construction of $\mathcal{F}\ell$ requires a coupled system of $2N(N+1)$ linear and nonlinear ODEs to be solved numerically. Of course, the transformation to co-rotating coordinates, and the consequent simplification of the Floquet problem, are only possible because we are considering anisotropic spin chains which retain a $SO(2)$ isotropy group. The technique will not work in chains with fully anisotropic exchange interaction, as are considered in [9].

The numerical results described below were obtained by computing spec $\Lambda$ using various standard routines taken from [15] on a 41-site lattice (the results do not differ significantly from those obtained with an 81-site lattice). It should be noted that, while the algorithm to construct the breather initial profile $\theta$ employed spatial reflexion symmetry, no such symmetry is imposed on the spectral problem for $\Lambda$. Hence *all* possible modes of instability are included in the analysis. Given the spectrum $\{\lambda_i\}$ of $\Lambda$, one constructs

$$\mu := \max_i (\mathrm{Re}\,\lambda_i)^2. \tag{5.20}$$

The corresponding breather is stable if and only if $\mu = 0$.

Figure 10 presents a graph of the maximal $\tilde{\alpha}(\omega)$ of theorem 2, that is, the coupling at which instability of the frequency $\omega$ ($o$+)-breather first occurs. Three features should be noted. The first is that, contrary to expectation, weakly coupled breathers remain stable even at resonant frequencies, $\omega^{-1} \in \mathbb{Z}$. In fact, there seems to be nothing special about these frequencies at all from the standpoint either of breather existence (see sections 3 and 4) or of stability. Second, $\tilde{\alpha}(\omega)$ appears to be finite for all $\omega$: even when $\omega > 0.424$ so that the ($o$+)-breather continues all the way to the continuum soliton (a linearly stable solution of the continuum system), it loses stability along the way. Third $\tilde{\alpha}(\omega)$ varies very little with $\omega$ except for $\omega$ close to unity. It appears to grow unbounded as $\omega \to 1$, which seems reasonable since the $\omega = 1$ ($o$+)-'breather' is nothing but the trivial vacuum $\boldsymbol{n}_i = \boldsymbol{e}_3$, which is stable for all $\alpha$. This limit is numerically inaccessible, however (the breathers tend to spread out over the whole lattice as $\omega$ grows so that finite-size effects dominate), so one should treat this observation with caution.

Figure 11 shows plots of $\mu$ against coupling $\alpha$ for ($o$+)-breathers of various frequencies. For $\omega \ll 0.424$, the breather remains stable until after it has joined the ($-$+) branch, only losing stability when this trivial static solution does. After this, $\mu$ grows monotonically with $\alpha$. For $\omega > 0.424$ the breather first loses and then regains stability: a hump of compact support appears in the graph of $\mu$. This hump is followed by another of roughly the same width but much less tall (note the change in vertical scale), so that stability is once again lost and regained. This leads us to conjecture that instability occurs in regularly repeating bands, the degree of instability (the height of the humps) decaying exponentially as $\alpha$ increases and the breather approaches the continuum soliton. It is interesting to note that the transition from stability to instability (or vice versa) generically coincides with a sign change in the determinant of $D\hat{F}$, where $\hat{F}$ is the *unsymmetrized* finite lattice version of the continuation function $F$ defined in (3.2). However no such sign change occurs in the Jacobian of the

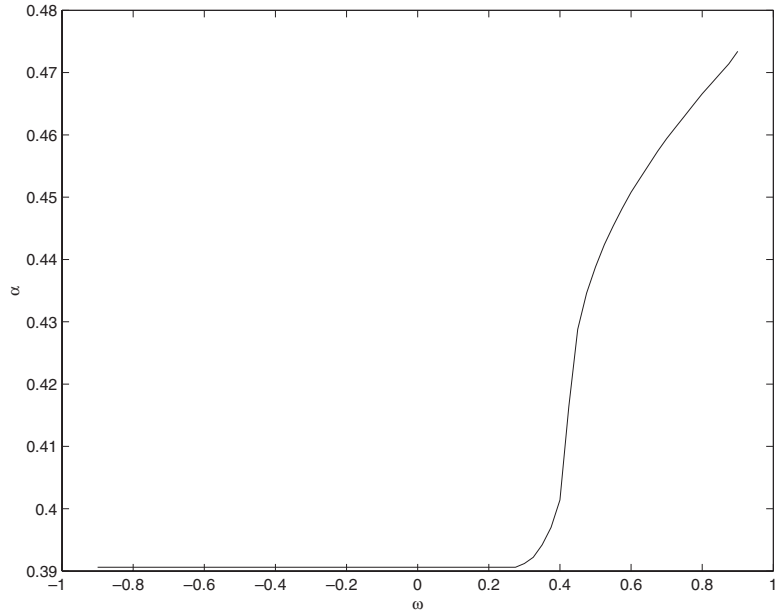


**Figure 10.** The coupling of first instability $\tilde{\alpha}$ as a function of frequency, $\omega$ for $(o+)$-breathers.

*symmetrized* continuation function (4.1), as employed in our continuation scheme, so the corresponding eigenvector $\delta\theta \in \ker D\hat{F}$ must have odd spatial parity. It seems likely, therefore, that stability transitions generically accompany symmetry breaking bifurcations in the full (i.e. unsymmetrized) continuation problem.

Figure 12 shows similar plots for $(-o+)$-breathers. Recall that no result equivalent to theorem 2 holds in this context, so there is no reason to expect stability even for arbitrarily small $\alpha$. Indeed, we found that for all $\omega$, $\mu$ departs from 0 as soon as $\alpha$ does. For $\omega \notin (0.133, 0.424)$ the breather remains unstable until it joins the appropriate trivial branch ($(--+)$ for $\omega < 0.133$, $(-+)$ for $\omega > 0.424$), whereupon it becomes briefly stable before instability irrevocably sets in. For $\omega \in (0.133, 0.424)$, the breathers gain stability, then lose it, rather in the fashion of the $(o+)$-breathers described above. Again, a pattern of repeating bands of diminishing instability seems to occur as $\alpha$ grows large and the breather approaches the continuum soliton. Plots of $\mu(\alpha)$ for $(--o+)$ breathers with $\omega \in (0.045, 0.133)$ are very similar: the breathers start as unstable, then gain and lose stability in a repetitive pattern. This leads us to conjecture that wherever breathers tend to the continuum soliton as $\alpha \to \infty$, a similar banded stability pattern occurs.

## 6. Conclusion

In this paper we have proved the existence of discrete breathers in ferromagnetic spin chains with easy-axis anisotropy, and constructed such breathers by means of numerical analysis. The main novelty of our numerical results is that discrete breathers exist independent of the inter-spin coupling $\alpha$, right up to the continuum limit $\alpha \to \infty$. This should be contrasted with previous studies of spin chains with easy-plane anisotropy [17], where the breathers are again 'monochromatic', but the spin waves have a different dispersion relation, and apparently do cause trouble at large $\alpha$.

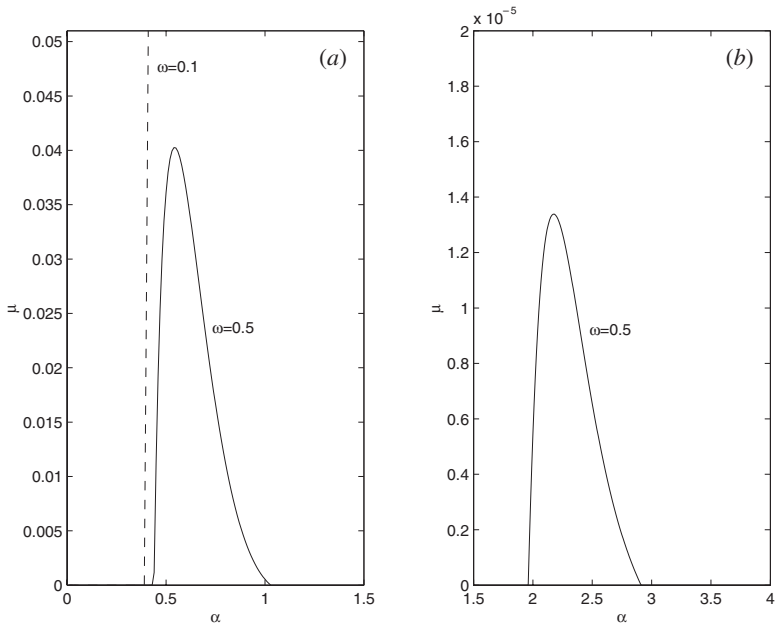


**Figure 11.** The instability function $\mu(\alpha)$, as defined in equation (5.20) for various ($o$+)-breathers (solid, $\omega = 0.5$; dashed, $\omega = 0.1$). The breather is stable if and only if $\mu = 0$. Note that both are stable for small $\alpha$ despite having resonant frequencies.

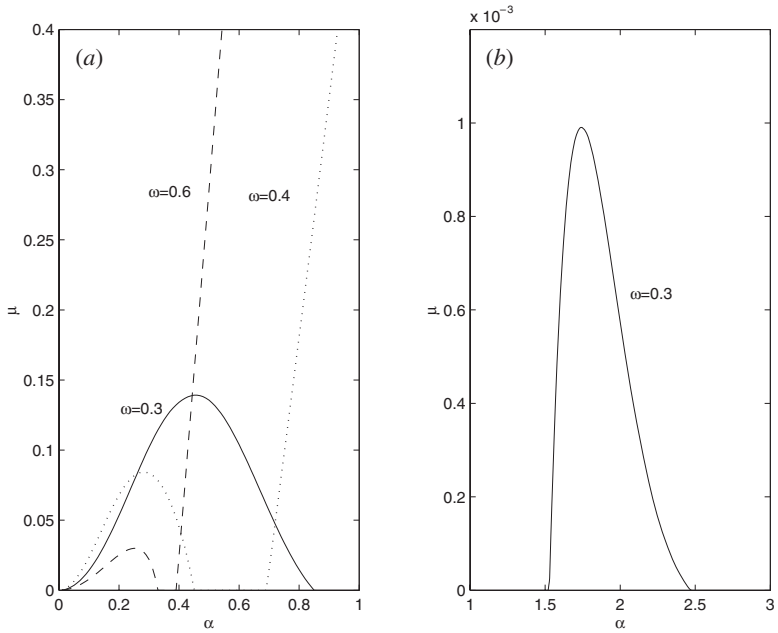


**Figure 12.** The instability function $\mu(\alpha)$ for various ($-o$+)-breathers (solid, $\omega = 0.3$; dashed, $\omega = 0.6$; dotted, $\omega = -0.4$). All are unstable for small $\alpha$, though they have nonresonant frequency.

The method of proof itself was something of a hybrid: an ansatz was made to reduce the equation for breathers from a system of ODEs to a purely algebraic system, but then existence of solutions of the latter was proved by continuing a decoupled solution in the sequence space $\ell_2$. Consequently, the result shares nice properties of both the Flach and MacKay–Aubry approaches. Since the reduced system depends parametrically on $\omega$, spin wave resonances cause no problems, theoretical or numerical (cf [13]). On the other hand, the result generalizes immediately to multi-dimensional spin lattices, as MacKay–Aubry style theorems usually do. Whether our numerical results generalize similarly, that is, whether a picture similar to figure 5 emerges for two- and three-dimensional lattices is an interesting open question. It should be noted that the continuum theory in higher dimensions does support radially symmetric, exponentially localized soliton solutions of the form analogous to (2.8), namely

$$\boldsymbol{n}(\boldsymbol{x}, t) = (\sin\theta(|\boldsymbol{x}|)\cos\omega t, -\sin\theta(|\boldsymbol{x}|)\sin\omega t, \cos\theta(|\boldsymbol{x}|)) \tag{6.1}$$

although explicit expressions for $\theta(r)$ are not known [11].

The ansatz may be interpreted as transforming to co-rotating coordinates, wherein the breather solutions are static. This viewpoint greatly simplifies the linear stability analysis since one need only solve an autonomous linear system of ODEs. In this way we have made an extensive study of the linear stability properties of the breathers. The results suggest that those breather families which converge as $\alpha \to \infty$ to the continuum soliton experience repeating bands of instability of diminishing strength as $\alpha$ increases. We found that the spin waves have no influence whatsoever on stability issues, even though the stability analysis includes all possible perturbations, including those *outside* the monochromatic ansatz. Flach *et al* [9] also perform a numerical linear stability analysis for breathers in their spin chains, and obtain results broadly similar to ours, namely one-site breathers are found to be stable at weak coupling, and certain multisite breathers are found to be unstable at weak coupling. The subsequent loss and regaining of (in)stability for increasing coupling is not reported—perhaps it is special to chains with isotropic exchange interaction. Their survey of the breather existence domains is rather less extensive than ours, however, presumably due to the much higher computational cost in their systems, so it is possible that similar band structures to those found here exist there also.

One open question immediately arises: that of breather mobility in this system. In the continuum limit, there exist travelling solitons which propagate at constant speed [11]. Can one find analogous propagating breathers at finite coupling? There seems to be little hope of proving anything rigorously about such objects, but one could still hope to study breather mobility numerically, focusing on how breather mobility depends on $\omega$ and $\alpha$. For a survey of what is known about moving discrete breathers, see the review articles [8,12]. One striking observation by Aubry and Cretegny is that breather mobility may be associated with certain behaviour of the Floquet matrix [2]. In a one-parameter family of breathers (such as $\theta^\alpha$), mobility occurs precisely at a value, $\alpha'$ say, where a certain type of Krein bifurcation occurs: $\mathcal{F}\ell$ becomes defective and so-called 'marginal modes' appear (they span the orthogonal complement of the sum of the $\mathcal{F}\ell_{\alpha'}$ eigenspaces). Perturbing $\theta_{\alpha'}$ in the direction of such a marginal mode produces a slowly translating breather. So breather mobility seems to be naturally associated with transitions from linear stability to instability. It would be interesting to see whether the stability transitions observed in section 5 have such significance.

## Acknowledgments

We acknowledge the EPSRC for a Postdoctoral Research Fellowship (JMS) and an Advanced Fellowship (PMS). One of us (JMS) would like to thank Chris Eilbeck for valuable conversations.

## References


[1] Aubry S 1997 Breathers in nonlinear lattices: existence, linear stability and quantization *Physica* D **103** 201

[2] Aubry S and Cretegny T 1998 Mobility and reactivity of discrete breathers *Physica* D **119** 34

[3] Baesens C and MacKay R S 1997 Exponential localization of linear response in networks with exponentially decaying coupling *Nonlinearity* **10** 931

[4] Choquet-Bruhat Y, DeWitt-Morette C and Dillard-Bleick M. 1982 *Analysis, Manifolds and Physics* Part I (Amsterdam: North-Holland) p 91

[5] Eilbeck J C, Lomdahl P S and Scott A C 1985 The discrete self-trapping equation *Physica* D **16** 318

[6] Carr J and Eilbeck J C 1985 Stability of stationary solutions of the discrete self-trapping equation *Phys. Lett.* A **109** 201

[7] Flach S 1995 Existence of localized excitations in nonlinear Hamiltonian lattices *Phys. Rev.* E **51** 1503

[8] Flach S and Willis C R 1998 Discrete breathers *Phys. Rep.* **295** 181

[9] Flach S, Zolotaryuk Y and Fleurov V 2001 Discrete breathers in classical spin lattices *Phys. Rev.* B **63** 214 422

[10] Johansson M and Kivshar Y S 1999 Discreteness-induced oscillatory instabilities of dark solitons *Phys. Rev. Lett.* **82** 85

[11] Kosevich A M, Ivanov B A and Kovalev A S 1990 Magnetic solitons *Phys. Rep.* **194** 117

[12] Lai R and Sievers A J 1999 Nonlinear nanoscale localization of magnetic excitations in atomic lattices *Phys. Rep.* **314** 147

[13] MacKay R S and Aubry S 1994 Proof of existence of breathers for time-reversible or Hamiltonian networks of weakly coupled oscillators *Nonlinearity* **7** 1623

[14] Marín J L and Aubry S 1996 Breathers in nonlinear lattices: numerical calculation from the anticontinuous limit *Nonlinearity* **9** 1501

[15] Press W H, Flannery B P, Teukolsky S A and Vetterling W T 1989 *Numerical Recipes* (Cambridge: Cambridge University Press) ch 11

[16] Sepulchre J A and Mackay R S 1997 Localized oscillations in conservative or dissipative networks of coupled autonomous oscillators *Nonlinearity* **10** 679

[17] Wallis R F, Mills D L and Boardman A D 1995 Intrinsic localized spin modes in ferromagnetic chains with on-site anisotropy *Phys. Rev.* B **52** R3828